pISSN 1598-2998, eISSN 2005-9256
https://doi.org/10.4143/crt.2021.843
Cancer Res Treat. 2022;54(3):782-792

Original Article

Selection Strategies and Practical Application of *BRAF* V600E-Mutated Non–Small Cell Lung Carcinoma

Inwoo Hwang[1], **Yoon-La Choi**[1,2,3], **Hyunwoo Lee**[1], **Soohyun Hwang**[1], **Boram Lee**[1,2], **Hobin Yang**[4], **Chaithanya Chelakkot**[5], **Joungho Han**[1]

[1]*Department of Pathology and Translational Genomics, Samsung Medical Center, Sungkyunkwan University School of Medicine, Seoul,* [2]*Samsung Advanced Institute of Health Science and Technology, Sungkyunkwan University School of Medicine, Seoul,* [3]*Laboratory of Cancer Genomics and Molecular Pathology, Samsung Medical Center, Seoul,* [4]*Research Institute of Pharmaceutical Sciences and College of Pharmacy, Seoul National University, Seoul,* [5]*Bio-MAX, Seoul National University, Seoul, Korea*

Purpose The incidence of *BRAF* V600E mutation in non–small cell lung carcinoma (NSCLC) is lower than 2%, which poses difficulties in finding legitimate patients for targeted therapy. We investigated the predictive factors pertaining to *BRAF* V600E and the effectiveness of the VE1 antibody as a screening method for patient selection.

Materials and Methods The study was designed into two steps. In a first group, *BRAF*-mutated NSCLCs were identified from sequencing data to determine the features of *BRAF* V600E mutation. The results of the first group helped the collection of adenocarcinomas with a papillary or micropapillary pattern but without epidermal growth factor receptor (*EGFR*) or anaplastic lymphoma kinase (*ALK*) alterations as a second group so that the frequency of *BRAF* V600E mutation could be calculated. The sensitivity and specificity of the VE1 were compared with *BRAF* V600E status.

Results Among 39 *BRAF*-mutated NSCLCs in the first group, 20 (51%) were V600E. *BRAF* V600E mutation was more common in female patients and showed no significant correlation with smoking status. Nineteen cases were adenocarcinomas without *EGFR* and *ALK* alterations. The most common patterns of invasion were papillary and micropapillary along with central fibrosis. The sensitivity and specificity of the VE1 were 90.0% and 92.3%, respectively. In the second group, 6.7% of cases were VE1-positive, indicating that the prevalence was significantly higher than that reported in previous studies (0.3%-1.8%).

Conclusion *BRAF* V600E-mutated NSCLCs could be enriched with the application of clinicopathologic parameters, which are not perfect. Therefore, additional VE1 immunohistochemistry may be useful as a screening method.

Key words *BRAF* V600E, Non-small-cell lung carcinoma, Adenocarcinoma of lung, Histology

Introduction

Lung cancer is the most common cause of cancer-related deaths worldwide. The mortality rate of lung cancer is still high, reaching approximately 23% and 22% in Korea and the United States, respectively [1,2]. *BRAF* mutation is one of the recently identified molecular targets to develop targeted therapies for non–small cell lung carcinoma (NSCLC). Dabrafenib either alone or in combination with trametinib has shown efficacy in *BRAF* V600E NSCLC, not otherwise specified or adenocarcinoma [3]. On this positive perspective, the National Comprehensive Cancer Network guideline recommends dabrafenib plus trametinib or vemurafenib/dabrafenib as the first-line treatment or the subsequent therapy followed by complete systemic therapy for advanced or metastatic NSCLCs with an identified *BRAF* V600E mutation [4]. The Food and Drug Administration concurrently approved the Oncomine Dx Target Test, the first next-generation sequencing (NGS) oncology panel test, to detect *BRAF* V600E among patients with NSCLC [5].

Despite their significance, *BRAF* mutations are rare genetic alterations in NSCLC, with a reported prevalence of 2.2%-8.9% in the Western population [6,7] and 0.5%-0.8% in the East Asian population [8,9]. Moreover, *BRAF* V600E accounts for only about 50% of *BRAF* mutations, posing difficulties in detection. NGS, polymerase chain reaction (PCR), including peptide nucleic acid clamping, real-time PCR, and droplet digital PCR, and Sanger sequencing are recommended for diagnosis; however, these techniques are more expensive than immunohistochemistry (IHC), given the rare incidence of this mutation.

Some studies have illustrated the clinical features of *BRAF* V600E-mutated NSCLC, but the histological features of this mutation remain unclear. Therefore, we aimed to investigate the most predictable conditions for *BRAF* V600E mutation. We conducted this study in two steps. In the first step, we

Correspondence: Yoon-La Choi
Department of Pathology and Translational Genomics, Samsung Medical Center, Sungkyunkwan University School of Medicine, Irwon-ro 81, Gangnam-gu, Seoul 06351, Korea
Tel: 82-2-3410-2800 Fax: 82-2-3410-6396 E-mail: ylachoi@skku.edu
Received July 25, 2021 **Accepted** October 18, 2021 **Published Online** November 23, 2021

found clinical characteristics, the most common histologic pattern and genetic feature of *BRAF* V600E as compared to other *BRAF*-mutated NSCLCs identified using NGS (a first group). In the second step (a second group), we investigated the frequency of *BRAF* V600E in surgical specimens collected based on the information from the first group. We also evaluated the sensitivity and specificity of the VE1 antibody (commercially available anti-*BRAF* V600E antibody) in the molecular screening method before the confirmative molecular test.

Materials and Methods

1. Patient selection

The experiment was designed into two steps. The purpose of the first step was to determine clinical characteristics, the most common histologic pattern, and epidermal growth factor receptor (*EGFR*) or anaplastic lymphoma kinase (*ALK*) alterations of *BRAF* V600E-mutated NSCLCs that were confirmed through NGS in the first group. We identified 42 (10.8%) *BRAF*-mutated NSCLC cases from 389 patients with NSCLC who were previously tested using targeted NGS, regardless of *BRAF* mutation types. The specimens were acquired through surgical resection, endobronchial ultrasound-guided transbronchial needle aspiration, or percutaneous core biopsy at the lung, regional lymph nodes, or distant metastasis sites and were analyzed using targeted NGS at Samsung Medical Center from January 2014 to May 2020. Among the 42 specimens, two specimens were eventually diagnosed with metastatic thyroid carcinoma of the lung and one specimen was obtained from the same patient at another distant metastatic site. Thus, 39 specimens were finally chosen for analysis, and two pathologists (I.H. and Y.-L.C.) carefully reviewed all the available slides. Clinical information, histological features, and *EGFR* and *ALK* alterations assessed by real-time PCR and IHC, respectively, were studied with confirmation of *BRAF* mutation type. As 14 of 39 *BRAF*-mutated specimens were adequate for evaluating invasion patterns, we also reviewed invasive patterns of these specimens.

In the second step, we determined the number of *BRAF* V600E mutations observed in the surgical specimens that met the criteria based on the findings identified in the first group. As a papillary or micropapillary pattern was the most common pattern and all *BRAF* V600E-mutated NSCLCs from the first group were negative for *EGFR* and *ALK* alterations, we next examined the frequency of *BRAF* V600E mutation from adenocarcinomas with a papillary or micropapillary pattern but without *EGFR* and *ALK* alterations in the second group. In a single center (Samsung Medical Center), between August 2016 and May 2019, 2,817 patients underwent lung surgery, including wedge resection, lobectomy, or pneumonectomy. Of these, only 56 patients with adenocarcinomas (2.0%) showed a predominant papillary or micropapillary pattern without *EGFR* and *ALK* alterations. Among papillary or micropapillary predominant adenocarcinomas in the first group, either a papillary or micropapillary pattern accounted for more than 30% of the total tumor volume; thus, the cutoff value for each papillary or micropapillary pattern in the second group was set to 30%. *EGFR* and *ALK* alterations in the second group were also tested using real-time PCR and

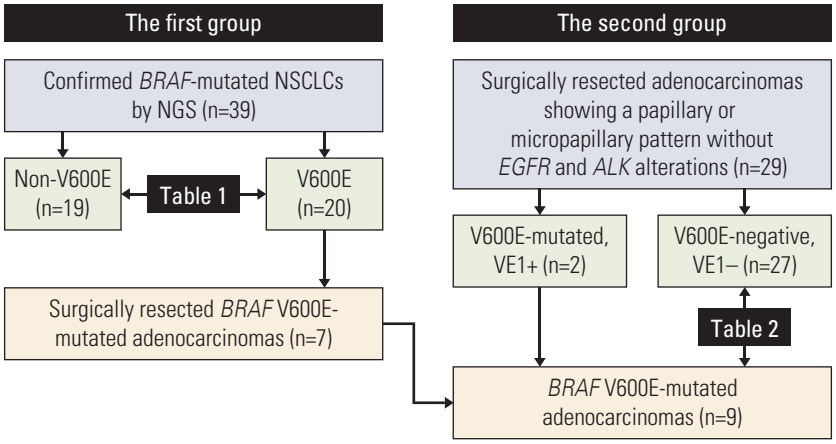

Fig. 1. Overview of the patient selection process (the excluded specimens are not described here). Two out of the 29 specimens (6.9%) were positive for VE1 immunohistochemistry based on our selection criteria. Due to the small number, the surgically resected specimens in the first and the second groups were analyzed together to determine the clinicopathologic features, which are presented in Table 2. ALK, anaplastic lymphoma kinase; EGFR, epidermal growth factor receptor; NGS, next-generation sequencing; NSCLC, non–small cell lung carcinoma.

IHC, respectively. Three patients were excluded because of a previous history of papillary thyroid carcinoma to avoid ambiguity. One case was removed from the second group, as the patient was already enrolled with biopsy in the first group. After careful review of the surgically resected specimens from 52 patients, 23 cases were excluded because only a minor portion (less than 30% of the entire tumor volume) presented a papillary or micropapillary pattern.

We performed immunostaining with the VE1 antibody on the remaining 29 specimens to detect *BRAF* V600E, and then subjected VE1-positive specimens to real-time PCR as a confirmatory method. We combined surgically resected specimens with *BRAF* V600E from the first group (7 cases) with *BRAF* V600E–mutated specimens from the second group (2 cases) for further analysis (Fig. 1). Clinical details were extracted from the medical records, and none of the patients had received targeted therapy.

2. Histological review

BRAF-mutated specimens from the first group were collected by either resection or biopsy, and all specimens from the second group were surgically resected. The biopsy specimens were thoroughly reviewed for all slides, and the resected specimens were also reviewed on all available representative slides. Two pathologists (I.H. and Y.-L.C.) were separately involved in the slide review, and in case of any discrepancy, the pathologists reviewed the slides together with mutual consent.

We recorded all patterns of invasion observed in pattern-recognizable specimens from the first group (14 cases) and all specimens from the second group at a 5% increment. The pattern of invasion was defined as follows: (1) a papillary pattern was defined as tertiary or more branched glandular tumor growth with a fibrovascular core; (2) a micropapillary pattern was defined as a pattern that formed papillary tufts without a fibrovascular core that were within the alveolar space, fibrous capsule, or embedded in the fibrous stroma. The filigree pattern was not distinguished from the micropapillary pattern; (3) a solid pattern was defined as polygonal cells arranged in sheets without lepidic, acinar, papillary, and micropapillary features; (4) infrequent patterns such as cribriform were considered as others.

Considering the lack of consensus regarding other histological features, we defined them in this study. The nuclear size was defined as intermediate or large when it was three or five times larger than the average lymphocyte diameter. We interpreted the nucleolus as prominent if it was easily seen under the low-power field (×100) or as inconspicuous if it could be observed under the high-power field (×400). Nuclear pleomorphism was determined by considering nuclear size and shape variation. Nuclear atypia was graded based on nuclear size, nucleoli, and nuclear pleomorphism. Central fibrosis and tumor-associated fibrosis were defined as fibrosis located in the central region of invasion and stromal fibroblasts running side by side with the tumor, respectively (S1 Fig.).

3. IHC with the VE1

To confirm the diagnostic value of the VE1 antibody, IHC was performed on all available specimens from the first group to verify both sensitivity and specificity. In the second group, the VE1 was tested as a screening method and then real-time PCR was performed as a confirmatory test to verify the screening value of the VE1.

Formalin-fixed paraffin–embedded (FFPE) tissue blocks were immediately prepared after receiving fresh specimens. Unstained slides were prepared by cutting 4 μm thick sections and staining using Ventana BenchMark ULTRA IHC/ISH (Ventana Medical Systems, Tucson, AZ) immunostainer. The specimens were incubated with the VE1 (mouse monoclonal primary antibody) for 16 mintues at 36°C, and the sections were visualized using OptiView DAB IHC v6, followed by hematoxylin II and eosin (H&E) counterstaining. Papillary thyroid carcinoma and colon adenocarcinoma tissues with *BRAF* V600E mutation were used as positive controls. IHC was interpreted by two pathologists (I.H. and Y.-L.C.) using a two-tier positive and negative system. In NSCLC, weak and focal staining was considered positive because the VE1 antibody tends to show weaker staining in NSCLC than in *BRAF*-mutated carcinomas of other organs.

4. DNA preparation, NGS, and real-time PCR

The tumor areas on H&E-stained slides were marked by a pathologist (I.H.), and the marked tumors from FFPE samples were cut into 10-μm sections. After deparaffinization with xylene (five times, 5 minutes each) and ethanol (twice, 5 minutes each), DNA extraction was performed using QIAamp DNA FFPE Tissue Kit (Qiagen, Hilden, Germany) and DNA quantification was carried out using a UV-VIS spectrophotometer.

NGS used in the first group selection included customized gene panels designed at the Samsung Medical Center. It covered selected gene variants associated with approved therapy, clinical trial in progress, or association with therapeutic responses in the public databases and the literature, including 83 genes in version 1 and 381 genes in version 2. The *BRAF* panel was designed to find single nucleotide variants (SNVs), small indels, and copy number variations (CNVs) in version 1, and SNVs/indels/CNVs plus fusion in version 2 for all exon regions. Sequencing of the targeted DNA was performed on the HiSeq2500 platform (Illumina, San Diego, CA).

Table 1. Clinical, genetical, and histological characteristics of *BRAF*-mutated lung cancer

Variable	Total (n=39)	Non-V600E (n=19)	V600E (n=20)	p-value
Age, mean (yr)	39	63.31	65.05	0.586
Sex				
Female	20	6 (31.6)	14 (70.0)	0.016
Male	19	13 (68.4)	6 (30.0)	
Smoking status				
Never smoker	23	9 (47.4)	14 (70.0)	0.137
Ex-smoker	10	5 (26.3)	5 (25.0)	
Current smoker	6	5 (26.3)	1 (5.0)	
Diagnosis				
Others	6	5 (26.3)	1 (5.0)	0.091
Adenocarcinoma	33	14 (73.7)	19 (95.0)	
***EGFR* alteration**				
Negative	30	10 (58.8)	20 (100)	0.002
Positive	7	7 (41.2)	0	
NA[a]	2	2	0	
***ALK* alteration**				
Negative	36	16 (94.1)	20 (100)	0.459
Positive	1	1 (5.9)	0	
NA[a]	2	2	0	
***BRAF* V600E IHC (VE1)**				
Negative	13	12 (92.3)	1 (10.0)	< 0.001
Positive	10	1 (7.7)	9 (90.0)	
NA[a]	16	6	10	
Primary pattern				
Acinar	1	1 (33.3)	0	0.110
Micropapillary	4	0	4 (36.4)	
Papillary	4	0	4 (36.4)	
Solid	5	2 (66.7)	3 (27.3)	
NA[b]	25	16	9	

Values are presented as number (%). ALK, anaplastic lymphoma kinase; EGFR, epidermal growth factor receptor; IHC, immunohistochemistry. [a]Data are not available; samples are insufficient for testing, [b]Data are not available; sample sizes are inappropriate for interpretation.

Real-time PCR was performed using the Real-Q *BRAF* V600E Detection Kit (BioSewoom, Seoul, Korea) comprising a reaction mixture and a *BRAF* probe and primer mixture according to the manufacturer's protocol. PCR was performed using ABI PRISM 7000/7300/7500/7900HT Real-Time PCR System (Applied Biosystems, Foster City, CA) as follows: denaturation at 95°C for 10 minutes after incubation at 50°C for 2 minutes, 40 cycles of amplification at 95°C for 15 seconds and extension at 58°C for 45 seconds. Fluorescence was detected after the last step of the cycle. The threshold of the internal control was 0.2 and that of *BRAF* was 0.03. The internal control Ct value was 27±4 cycles, and the sample was considered positive for *BRAF* V600E mutation if the Ct value of *BRAF* V600E was 24±4 cycles.

5. Statistical analysis

Data in this study that contained discontinuous (categorical) variables were analyzed using the Fischer exact test. Continuous variables were evaluated using an independent t test. The hazard ratios for overall survival (OS) and recurrence-free survival (RFS) between *BRAF* V600E-mutated and negative groups were estimated using the Kaplan-Meier methods. IBM SPSS Statistics for Windows ver. 27.0 (IBM Corp., Armonk, NY) was used for all statistical analyses.

Results

In the first group, approximately half of *BRAF*-mutated NSCLCs (20/39, 51.3%) harbored *BRAF* V600E mutation

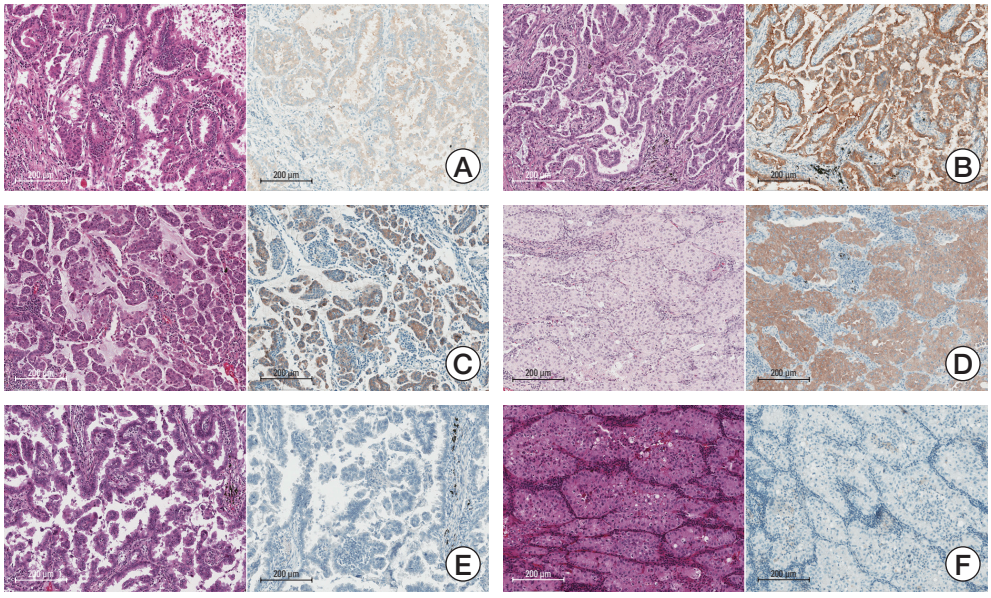

Fig. 2. Various invasive patterns of adenocarcinoma with or without *BRAF* V600E mutation. (A) Acinar pattern. The entire sections of this tumor showed micropapillary and papillary predominant patterns with focal (less than 30%) acinar patterns. VE1 immunohistochemistry (IHC) was weak positive and *BRAF* V600E was confirmed by real-time polymerase chain reaction. (B) Most areas of this adenocarcinoma showed a papillary pattern. A micropapillary pattern was also presented but not predominant. VE1 antibody staining was strong positive. (C) A micropapillary dominant adenocarcinoma. The tumor also had a focal acinar pattern within central fibrosis (not shown), but the area's volume did not exceed 30% of the total volume. VE1 IHC was diffuse and intermediate to strong positive. (D) The adenocarcinoma was mainly composed of a solid pattern. The tumor had high-grade nuclear atypia with abundant pale eosinophilic cytoplasm, and the stroma showed dense lymphocytic infiltration. VE1 IHC was diffuse and strong positive. (E) *BRAF* V600E–negative adenocarcinoma with papillary and micropapillary patterns. VE1 immunostaining was negative. (F) Solid pattern with VE1-negative staining (A-F, H&E staining and VE1 immunostaining, scale bar=200 μm).

(Table 1; raw data shown in S2 Table). There was no significant difference in the smoking status among patients with *BRAF* V600E mutation and those with *BRAF* non-V600E mutation (p=0.137), but *BRAF* V600E mutation was significantly more common among female patients than among male patients (p=0.016). All *BRAF* V600E–mutated cases, except one, were diagnosed with adenocarcinoma (Fig. 2). *EGFR* and *ALK* alterations were not identified in any *BRAF* V600E-mutated NSCLC but was detected in *BRAF* non-V600E-mutated NSCLCs (41.2% [7/17] and 5.9% [1/17], respectively). Histologically, papillary (36.4%, 4/11) and micropapillary (36.4%, 4/11) patterns were predominant (Fig. 2B and C), followed by solid pattern (27.3%, 3/11) (Fig. 2D). None of *BRAF* V600E–mutated adenocarcinomas showed acinar predominance, except one case with a secondary pattern (S3 Fig.). The sensitivity of the VE1 antibody was 90.0% (9/10) and its specificity was 92.3% (12/13).

Based on the first group's statistics, we collected recently resected lung adenocarcinomas with a papillary or micropapillary pattern but without *EGFR* and *ALK* alterations in the second group. We screened 29 among 2,817 cases and found two (6.9%, 2/29) cases as VE1-positive; *BRAF* V600E in these cases was confirmed by real-time PCR.

After combining the available resected specimens from the first (7 cases) and the second (2 cases) group, clinical and histological characteristics were analyzed. In comparison to *BRAF* V600E–negative adenocarcinomas showing a papillary or micropapillary pattern without *EGFR* and *ALK* alterations, *BRAF* V600E–mutated adenocarcinomas had a significantly different desmoplastic pattern; central fibrosis was more common in *BRAF* V600E (p=0.046, Table 2; raw data shown in S4 Table). However, lymphovascular invasion, pleural invasion, spread through air spaces, nuclear atypia, and other histological features were not significantly different between the two groups. Clinically, age, smoking status, and initial stage did not significantly differ; however, *BRAF* V600E mutation was more common in women than in men (p=0.012), consistent with the first group's result. RFS and OS were not significantly different between *BRAF* V600E-mutated and negative patients (RFS, p=0.146; OS, p=0.782) (Fig. 3).

Table 2. Histological and clinical characteristics of *BRAF* V600E-mutated lung adenocarcinoma

Variable	*BRAF* V600E		p-value
	Absent	Present	
Histological feature			
Lymphovascular invasion			
Absent	17 (63.0)	3 (33.3)	0.146
Present	10 (37.0)	6 (66.7)	
Pleural invasion			
PL0	15 (55.6)	6 (66.7)	0.688
PL1	3 (11.1)	2 (22.2)	
PL2	7 (25.9)	1 (11.1)	
PL3	2 (7.4)	0	
Spread through air spaces			
Absent	14 (51.9)	3 (33.3)	0.451
Present	13 (48.1)	6 (66.7)	
Desmoplastic pattern			
Absent	11 (40.7)	3 (33.3)	0.046
Central fibrosis	7 (25.9)	6 (66.7)	
Tumor-associated fibrosis	9 (33.3)	0	
Nuclear atypia			
Low	1 (3.7)	0	> 0.99
Intermediate	20 (74.1)	7 (77.8)	
High	6 (22.2)	2 (22.2)	
Nuclear size			
Small	1 (3.7)	0	0.665
Intermediate	22 (81.5)	9 (100)	
Large	4 (14.8)	0	
Nuclear pleomorphism			
Low	17 (63.0)	7 (77.8)	0.685
High	10 (37.0)	2 (22.2)	
Nucleoli			
Absent	1 (3.7)	0	0.097
Inconspicuous	13 (48.1)	1 (11.1)	
Prominent	13 (48.1)	8 (88.9)	
Mucin-containing cells			
Absent	12 (44.4)	2 (22.2)	0.076
Focal	9 (33.3)	7 (77.8)	
Diffuse	6 (22.2)	0	
Nuclear pseudoinclusion			
Absent	20 (74.1)	7 (77.8)	> 0.99
Present	7 (25.9)	2 (22.2)	
Psammomatous calcification			
Absent	24 (88.9)	8 (88.9)	> 0.99
Present	3 (11.1)	1 (11.1)	
Nuclear groove			
Absent	24 (88.9)	8 (88.9)	> 0.99
Present	3 (11.1)	1 (11.1)	

(Continued to the next page)

Table 2. Continued

Variable	*BRAF* V600E		p-value
	Absent	Present	
Clinical feature			
Age, mean (yr)	63.52	67.00	0.443
Sex			
Female	5 (18.5)	6 (66.7)	0.012
Male	22 (81.5)	3 (33.3)	
Smoking status			
Never smoker	9 (33.3)	6 (66.7)	0.286
Previous smoker	11 (40.7)	2 (22.2)	
Current smoker	7 (25.9)	1 (11.1)	
Stage			
IA	6 (22.2)	0	0.379
IB	2 (7.4)	1 (11.1)	
IIA	0	1 (11.1)	
IIB	4 (14.8)	2 (22.2)	
IIIA	8 (29.6)	2 (22.2)	
IIIB	4 (14.8)	3 (33.3)	
IVA	2 (7.4)	0	
IVB	1 (3.7)	0	

Values are presented as number (%).

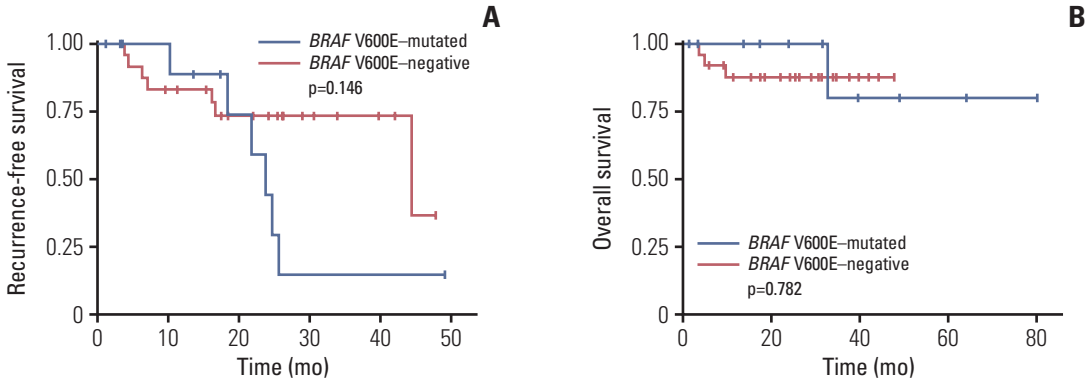

Fig. 3. The recurrence-free survival (A) and overall survival (B) of *BRAF* V600E–mutated and V600E–negative adenocarcinomas with a papillary or micropapillary pattern but without epidermal growth factor receptor (*EGFR*) and anaplastic lymphoma kinase (*ALK*) alterations. After surgical resection, there was no difference in the recurrence-free survival and overall survival between *BRAF* V600E–mutated and V600E–negative adenocarcinomas (recurrence-free survival, p=0.146; overall survival, p=0.782).

Discussion

BRAF mutations are classified as class I, II, and III based on the kinase activity, RAS dependency, and dimerization status. *BRAF* V600E is a class I *BRAF* mutation that strongly activates kinase activity, thereby stimulating the downstream *MEK-ERK* pathway [10]. Dual inhibitors of *BRAF* and *MEK* showed 64% (23/36) overall response in a multicohort, multicenter, non-randomized, open-labeled clinical trial of adult patients with metastatic *BRAF* V600E-mutated NSCLC (NCT01336634) [11]. A combination of a *BRAF* inhibitor (dabrafenib) and a *MEK* inhibitor (trametinib) has been approved and was found to significantly improve the survival of patients with advanced NSCLC harboring *BRAF* V600E mutation.

Despite the high efficacy of *BRAF*-targeted therapies, it is difficult to choose the appropriate patient group because of its low incidence. While pre-invasive lung lesions commonly

have class II or class III *BRAF* mutations [12,13], 2.2%-8.9% of NSCLCs have *BRAF* mutations in the Western population; as per data, about 50%-57% of them have class I *BRAF* (V600E) mutation [6,7,14-17]. The lower incidence of *BRAF* mutations in the East Asian population (0.5%-0.8%) poses difficulties in finding patients with *BRAF* V600E to provide appropriate treatment [8,9]. Therefore, it is imperative to develop cost-effective strategies and methods for *BRAF* V600E screening.

To determine the features of *BRAF* V600E–mutated adenocarcinomas, we compared the clinical, histologic, and genetic features between *BRAF* V600E and non-V600E NSCLCs in the first step and between *BRAF* V600E and V600E-negative adenocarcinomas in the second step. The higher frequency of *BRAF* V600E in women than in men observed in our study (p=0.016) (Table 1) was similar to that reported by Marchetti et al. [14]. However, other studies reported no difference in V600E-mutated adenocarcinomas between men and women [6,18]. Although no statistical significance was observed with the smoking status, *BRAF* V600E–mutated adenocarcinoma was more likely to occur in never smokers than ever smokers (p=0.137). Some researchers suggested that *BRAF*-related tumor initiation of atypical adenomatous hyperplasia and adenocarcinoma was not related to smoking history unlike *KRAS* mutation [6,14], while Paik et al. [19] reported that all patients with *BRAF*-mutated adenocarcinomas were current or former smokers regardless of the cancer stage. It should be considered that the smoking rate of *BRAF* V600E-mutated adenocarcinoma may be affected by the smoking rate of the studied population.

The prognostic impact of *BRAF* V600E is also controversial, as some data suggested an association between *BRAF* V600E and poor progression-free survival and OS [6,14] and Dagogo-Jack et al. [20] reported a more aggressive behavior of non-V600E than of V600E in a large cohort. In our study, there was no difference in postoperative OS and RFS between *BRAF* V600E-mutated and negative adenocarcinomas with a micropapillary or papillary pattern but without *EGFR* and *ALK* alterations.

EGFR and *ALK* alterations were not accompanied by *BRAF* V600E in our first group, whereas driver mutations were observed in *BRAF* non-V600E patients. In a meta-analysis, the co-occurrence of *EGFR* and *BRAF* alterations was reported in 0.1% adenocarcinomas (2/1,929) in the Western population but was not observed (0/321) in the Asian population regardless of *BRAF* mutations [21]. However, Li et al. [8] reported *EGFR* and *BRAF* V600E co-mutations in two out of 26 cases; hence, *BRAF* V600E and *EGFR* co-mutations cannot be completely excluded.

Histologically, *BRAF* mutations could occur in adenocarcinomas, squamous cell carcinomas, poorly differentiated carcinomas, and others. Considering *BRAF* V600E, almost all histologic types were adenocarcinomas except one case; this observation is consistent with that previously reported [14,17]. Morphological variations were also observed with *BRAF* V600E mutation, including acinar, papillary, solid, and micropapillary patterns; however, *BRAF* V600E-mutated adenocarcinomas usually exhibited a papillary or micropapillary pattern at least in the focal region. As the predominant patterns of *BRAF* V600E adenocarcinomas in our study were papillary, micropapillary, and solid patterns, a non-acinar predominant pattern was more common than an acinar/lepidic predominant pattern. Considering all patterns that exceeded 30% of the overall tumor volume, micropapillary and papillary patterns were more frequent and comprised 6/11 and 6/11 cases, respectively; on the other hand, a solid pattern was observed in 3/11 cases, which was also consistent with observations from earlier studies [6,22]. Even in adenocarcinomas with a solid or acinar pattern, a papillary or micropapillary pattern tended to be present as a secondary or tertiary pattern.

Considering the histologic and genetic features of the first group, we collected surgically resected adenocarcinomas that had a papillary or micropapillary pattern in at least 30% of the overall tumor volume but without *EGFR* and *ALK* alterations. Under these conditions, the prevalence of *BRAF* V600E mutation was much higher (2/29, 6.9%) than that previously reported in the East Asian population (0.3%-0.5% of NSCLC [8,9] and 1.8% of stage III/IV adenocarcinoma without *EGFR* and *ALK* alterations [23]). The percentage would even increase up to 10% (3/30), considering that one case in the second group was excluded owing to the overlap with the first group. Further, the only histological feature of *BRAF* V600E was a desmoplastic pattern, especially central fibrosis. Although central fibrosis is known for poor prognosis and frequent lymphovascular invasion [24], the prognostic effect of the tumor microenvironment by *BRAF* V600E's central fibrosis is limited considering that tumor-associated fibrosis also provides a fibrotic background ($p > 0.99$) and there was no significant difference in lymphovascular invasion (p=0.146). This feature, however, can be helpful when evaluating *BRAF* V600E-mutated adenocarcinomas under light microscopy.

The gold standard method for detecting *BRAF* V600E is DNA-based techniques such as direct sequencing, NGS, and PCR. According to a study by Harle et al. [25], the sensitivity of real-time allele-specific amplification (RT-ASA) and IHC as compared to that of NGS in metastatic melanoma was 93.5% and 81.7%, respectively, and the specificity was 100%. However, when only V600E was targeted, the concordance rate of NGS, RT-ASA, and IHC was 100%. DNA-based tests can be affected by inappropriate sample conditions, such as low tumor volume, extensive necrosis, sustained ischemia,

or improper fixation. However, even in such cases, IHC can confirm the results if any positive cells are present. Given this practical situation, it would be important to consider that DNA-based tests may be false-negative depending on the tissue condition.

The VE1 antibody was known to have a sensitivity of 82%-100% and a specificity of 95.2%-100% in detecting *BRAF* V600E mutation [26,27]. We also verified good sensitivity (90%) and specificity (92%) of the VE1 antibody. IHC is widely used by pathologists because it is relatively easy to perform and interpret, and has a short turnaround time. Therefore, IHC can be suitable as a screening tool for *BRAF* V600E-mutated NSCLC before performing further definitive tests such as NGS, direct sequencing, or PCR. However, the interpretation of IHC requires close attention because the VE1 staining in NSCLC tends to be weak and focal. While interpreting the VE1 immunostaining in lung cancer, cross-reactivity at the bronchial airway can be used as a positive internal control because the VE1 shows strong staining in the axonemal dynein heavy chain [28].

The solid pattern was not investigated in this study because the main objective of this study was to find the most predictable *BRAF* V600E characteristics in surgical specimens. However, some researchers reported the solid pattern as the most common or second most common pattern, and we also observed it as the second most common pattern [7,22]. In our further investigation, we collected another 31 adenocarcinomas without *EGFR* and *ALK* alterations but with a solid pattern in at least 30% of the total tumor volume. The VE1 IHC staining was performed, and two out of 31 (6.5%) were VE1-positive (data not shown). After reviewing these cases, one showed solid and papillary patterns accounting for 40% and 30%, respectively, and the other had 50% of a solid pattern and 50% of a micropapillary pattern (S5 Fig.).

Another restriction of *BRAF*-mutated NSCLC studies is statistical difficulties, owing to the low incidence and heterogeneity of *BRAF* mutations. As discussed earlier, this issue leads to different clinical and prognostic outcomes of *BRAF*-mutated NSCLC in different studies. Similarly, in this study, as the number of patients was small, the possibility of false negatives originating from conservative statistics cannot be completely excluded. In addition, the statistics in Table 2 were performed by combining the first and second groups due to insufficient sample size. As many specimens in Table 2 were derived from samples that have already been tested for NGS, there may be an unknown selection bias. It should also be noted that the comparison group for the first step was *BRAF* non-V600E group and that for the second step was *BRAF* V600E–negative group.

In summary, our findings indicate that *BRAF* V600E–mutated NSCLC is more likely to occur in women and is diagnosed with adenocarcinoma, probably regardless of the smoking status. *EGFR* and *ALK* alterations may be mutually exclusive in *BRAF* V600E. Histologically, papillary and micropapillary patterns are predominant in *BRAF* V600E-mutated adenocarcinomas, but various other patterns can also be observed. Central fibrosis provides helpful insights for light microscopy screening. The VE1 antibody shows potency as a screening tool in patient selection. The histological and clinical features of *BRAF* V600E are not easy to differentiate, and it is essential to improve diagnostic methods for patients with *BRAF* V600E mutation to provide efficient therapeutic options.

Electronic Supplementary Material

Supplementary materials are available at Cancer Research and Treatment website (https://www.e-crt.org).

Ethical Statement

This study was approved by the Institutional Review Board of Samsung Medical Center with a waiver of informed consent (IRB No.2021-07-113-001) and conducted according to the principles of the Declaration of Helsinki.

Author Contributions

Conceived and designed the analysis: Hwang I, Choi YL, Han J.
Collected the data: Hwang I, Lee B, Choi YL, Han J.
Contributed data or analysis tools: Hwang I, Lee B, Choi YL.
Performed the analysis: Hwang I, Choi YL.
Wrote the paper: Hwang I, Choi YL.
Critical revision of the manuscript for important intellectual content: Lee H, Hwang S, Yang H, Chelakkot C, Han J.
Supervision: Han J.

ORCID iDs

Inwoo Hwang : https://orcid.org/0000-0002-7749-3929
Yoon-La Choi : https://orcid.org/0000-0002-5788-5140

Conflicts of Interest

Conflict of interest relevant to this article was not reported.

Acknowledgments

This work was supported by the R&D Program of the Society of the National Research Foundation funded by the Ministry of Science, ICT & Future Planning (NFR-2019R1A2B5B02069979 and MRC:2016R1A5A2945889).

References

1. Hong S, Won YJ, Park YR, Jung KW, Kong HJ, Lee ES, et al. Cancer statistics in Korea: incidence, mortality, survival, and prevalence in 2017. Cancer Res Treat. 2020;52:335-50.
2. Siegel RL, Miller KD, Fuchs HE, Jemal A. Cancer statistics, 2021. CA Cancer J Clin. 2021;71:7-33.
3. Khunger A, Khunger M, Velcheti V. Dabrafenib in combination with trametinib in the treatment of patients with BRAF V600-positive advanced or metastatic non-small cell lung cancer: clinical evidence and experience. Ther Adv Respir Dis. 2018;12:1753466618767611.
4. Ettinger DS, Wood DE, Aisner DL, Akerley W, Bauman JR, Bharat A, et al. NCCN guidelines insights: non-small cell lung cancer, version 2.2021. J Natl Compr Canc Netw. 2021;19:254-66.
5. Odogwu L, Mathieu L, Blumenthal G, Larkins E, Goldberg KB, Griffin N, et al. FDA approval summary: dabrafenib and trametinib for the treatment of metastatic non-small cell lung cancers harboring BRAF V600E mutations. Oncologist. 2018;23:740-5.
6. Ilie M, Long E, Hofman V, Dadone B, Marquette CH, Mouroux J, et al. Diagnostic value of immunohistochemistry for the detection of the BRAFV600E mutation in primary lung adenocarcinoma Caucasian patients. Ann Oncol. 2013;24:742-8.
7. Villaruz LC, Socinski MA, Abberbock S, Berry LD, Johnson BE, Kwiatkowski DJ, et al. Clinicopathologic features and outcomes of patients with lung adenocarcinomas harboring BRAF mutations in the Lung Cancer Mutation Consortium. Cancer. 2015;121:448-56.
8. Li S, Li L, Zhu Y, Huang C, Qin Y, Liu H, et al. Coexistence of EGFR with KRAS, or BRAF, or PIK3CA somatic mutations in lung cancer: a comprehensive mutation profiling from 5125 Chinese cohorts. Br J Cancer. 2014;110:2812-20.
9. Kobayashi M, Sonobe M, Takahashi T, Yoshizawa A, Ishikawa M, Kikuchi R, et al. Clinical significance of BRAF gene mutations in patients with non-small cell lung cancer. Anticancer Res. 2011;31:4619-23.
10. Yao Z, Yaeger R, Rodrik-Outmezguine VS, Tao A, Torres NM, Chang MT, et al. Tumours with class 3 BRAF mutants are sensitive to the inhibition of activated RAS. Nature. 2017;548:234-8.
11. Planchard D, Smit EF, Groen HJ, Mazieres J, Besse B, Helland A, et al. Dabrafenib plus trametinib in patients with previously untreated BRAF(V600E)-mutant metastatic non-small-cell lung cancer: an open-label, phase 2 trial. Lancet Oncol. 2017;18:1307-16.
12. Sivakumar S, Lucas FA, McDowell TL, Lang W, Xu L, Fujimoto J, et al. Genomic landscape of atypical adenomatous hyperplasia reveals divergent modes to lung adenocarcinoma. Cancer Res. 2017;77:6119-30.
13. Kobayashi Y, Ambrogio C, Mitsudomi T. Ground-glass nodules of the lung in never-smokers and smokers: clinical and genetic insights. Transl Lung Cancer Res. 2018;7:487-97.
14. Marchetti A, Felicioni L, Malatesta S, Grazia Sciarrotta M, Guetti L, Chella A, et al. Clinical features and outcome of patients with non-small-cell lung cancer harboring BRAF mutations. J Clin Oncol. 2011;29:3574-9.
15. Litvak AM, Paik PK, Woo KM, Sima CS, Hellmann MD, Arcila ME, et al. Clinical characteristics and course of 63 patients with BRAF mutant lung cancers. J Thorac Oncol. 2014;9:1669-74.
16. Tissot C, Couraud S, Tanguy R, Bringuier PP, Girard N, Souquet PJ. Clinical characteristics and outcome of patients with lung cancer harboring BRAF mutations. Lung Cancer. 2016;91:23-8.
17. Cardarella S, Ogino A, Nishino M, Butaney M, Shen J, Lydon C, et al. Clinical, pathologic, and biologic features associated with BRAF mutations in non-small cell lung cancer. Clin Cancer Res. 2013;19:4532-40.
18. Gow CH, Hsieh MS, Lin YT, Liu YN, Shih JY. Validation of immunohistochemistry for the detection of BRAF V600E-mutated lung adenocarcinomas. Cancers (Basel). 2019;11:866.
19. Paik PK, Arcila ME, Fara M, Sima CS, Miller VA, Kris MG, et al. Clinical characteristics of patients with lung adenocarcinomas harboring BRAF mutations. J Clin Oncol. 2011;29:2046-51.
20. Dagogo-Jack I, Martinez P, Yeap BY, Ambrogio C, Ferris LA, Lydon C, et al. Impact of BRAF mutation class on disease characteristics and clinical outcomes in BRAF-mutant lung cancer. Clin Cancer Res. 2019;25:158-65.
21. Dearden S, Stevens J, Wu YL, Blowers D. Mutation incidence and coincidence in non small-cell lung cancer: meta-analyses by ethnicity and histology (mutMap). Ann Oncol. 2013;24:2371-6.
22. Yousem SA, Nikiforova M, Nikiforov Y. The histopathology of BRAF-V600E-mutated lung adenocarcinoma. Am J Surg Pathol. 2008;32:1317-21.
23. Kim HC, Kang YR, Ji W, Kim YJ, Yoon S, Lee JC, et al. Frequency and clinical features of BRAF mutations among patients with stage III/IV lung adenocarcinoma without EGFR/ALK aberrations. Onco Targets Ther. 2019;12:6045-52.
24. Suzuki K, Yokose T, Yoshida J, Nishimura M, Takahashi K, Nagai K, et al. Prognostic significance of the size of central fibrosis in peripheral adenocarcinoma of the lung. Ann Thorac Surg. 2000;69:893-7.
25. Harle A, Salleron J, Franczak C, Dubois C, Filhine-Tressarieu P, Leroux A, et al. Detection of BRAF mutations using a fully automated platform and comparison with high resolution melting, real-time allele specific amplification, immunohistochemistry and next generation sequencing assays, for patients with metastatic melanoma. PLoS One. 2016;11:e0153576.
26. Sasaki H, Shimizu S, Tani Y, Shitara M, Okuda K, Hikosaka Y, et al. Usefulness of immunohistochemistry for the detection of the BRAF V600E mutation in Japanese lung adenocarcinoma. Lung Cancer. 2013;82:51-4.
27. Hofman V, Benzaquen J, Heeke S, Lassalle S, Poudenx M, Long E, et al. Real-world assessment of the BRAF status in

non-squamous cell lung carcinoma using VE1 immunohistochemistry: a single laboratory experience (LPCE, Nice, France). Lung Cancer. 2020;145:58-62.
28. Jones RT, Abedalthagafi MS, Brahmandam M, Greenfield EA, Hoang MP, Louis DN, et al. Cross-reactivity of the BRAF VE1 antibody with epitopes in axonemal dyneins leads to staining of cilia. Mod Pathol. 2015;28:596-606.